Libyan Open University Journal of Applied Sciences (LOUJAS)
Volume 1 - Issue 2 - 2025 - Pages 66-76

Design and Performance Comparison of Bowtie and Bowtie-Slot Antennas for 10-GHz 6G Wireless Applications

Yahya Entiefa Mansour [1*], Abdaraouf Abdalla Ashuli [2], Eman Mohammed Alnegrat [3]
[1,2,3] Electrical Engineering Department, College of Technical Sciences, Bani Walid, Libya
***Email:** yahiqm22@gmail.com

تصميم ومقارنة أداء هوائيات Bowtie و Bowtie-Slot لتطبيقات الجيل السادس اللاسلكية بتردد 10 GHz

يحي إنتيفة منصور [1*]، عبد الرؤوف عبد الله السهولي [2]، إيمان محمد النقراط [3]
[3,2,1] قسم الهندسة الكهربائية، كلية العلوم التقنية، بني وليد، ليبيا

Received: 30-10-2025; Accepted: 11-12-2025; Published: 27-12-2025

Abstract:
In this paper, a compact bowtie antenna is presented. The evaluation of this design, including simulation and performance optimization, was conducted for operation at 10 GHz to support 6G wireless communication systems. The proposed antenna was implemented on a low relative permittivity substrate Duroid with a thickness of 1.27 mm, selected for its low dielectric loss and stable performance at millimeter-wave frequencies. A modified bowtie geometry is employed to enhance impedance matching, extend operational bandwidth, and improve radiation efficiency in the 8–12 GHz spectrum. Full-wave electromagnetic simulations are conducted using ANSYS HFSS to validate the antenna's return loss, gain, radiation pattern, and surface current distribution. Results demonstrate that the optimized bowtie structure achieves broadband operation with return loss below –10 dB around the 10 GHz resonance, making it a suitable candidate for compact 6G front-end devices, high-speed sensing, and short-range high-capacity links.

Keywords: millimeter-wave; Bowtie antenna; high gain; Ansys HFSS.

الملخص:
في هذه الورقة تم دراسة ومقارنة هوائي مدمج Bowtie مع هوائي BowtiSlot. تم تقييم هذا التصميم، بما في ذلك المحاكاة وتحسين الأداء، للعمل عند تردد 10 جيجا هرتز لدعم أنظمة الاتصالات اللاسلكية من الجيل السادس. تم تصميم الهوائي المقترح على ركيزة Duroid منخفضة السماحية النسبية بسمك 1.27 مم، والتي اختيرت لانخفاض فقد العازل وأدائها المستقر عند ترددات الموجات المليمترية. تم استخدام شكل هوائي Bowtie معدل لتحسين موائمة المعاوقة، وزيادة عرض النطاق الترددي، وتحسين كفاءة الإشعاع في طيف الترددات 8-12 جيجا هرتز. تم اجراء محاكاة للخصائص الكهرومغناطيسية للهوائي باستخدام برنامج ANSYS HFSS، للتحقق من صحة فقد الهوائي، وكسبه، ونمط إشعاعه، وتوزيع تيار السطح. تُظهر النتائج أن الهوائي BowtiSlot يحقق نطاق ترددي أكبر مع فقد أقل من -10 ديسيبل عند تردد رنين 10 جيجا هرتز، مما يجعله خيارا مناسبًا لأجهزة الجيل السادس المدمجة، والاستشعار عالي السرعة، والروابط قصيرة المدى عالية السعة.

الكلمات المفتاحية: موجة المليمتر؛ Bowtie antenna؛ كسب عالي؛ Ansys HFSS

Introduction

The rapid evolution toward Sixth-Generation (6G) communication systems introduces stringent requirements on antenna performance, including ultra-wide bandwidth, high data throughput, compact size, and low fabrication loss. Millimeter-wave operation in the X-band (8–12 GHz) and higher frequency ranges is of particular interest due to the availability of wide contiguous bandwidths that can support multi-gigabit wireless links, as highlighted in [1]. Within this context, the bowtie antenna has emerged as an effective solution because of its broadband

characteristics, planar profile, and ease of fabrication. Bowtie antennas are essentially flared, wideband variations of the classical dipole, and their geometry naturally supports a wide range of operating frequencies due to the gradual impedance transition along the triangular arms, as described in [2], [3], and [4]. This makes them attractive for high-frequency radar, imaging systems, and future 6G communication networks.

However, at millimeter-wave frequencies, careful optimization of the flare angle, arm length, feed gap, and substrate characteristics is required to maintain stable radiation behavior and minimize losses, which aligns with the design considerations [5], [6].

In this work, a bowtie antenna designed to resonate at 10 GHz is implemented on a 1.27 mm thick Rogers Duroid substrate, a material known for its low dielectric constant and minimal loss tangent. These material properties help reduce dielectric losses that typically degrade antenna performance at high frequencies, consistent with microstrip antenna theory [7], [8]. The antenna is modeled and analyzed using ANSYS HFSS 2025 R2 [9], where geometric modifications are applied to improve impedance matching and broaden the bandwidth suitable for 6G-class applications.

The objective of this study is to present a detailed design methodology, simulation analysis, and performance validation of a compact bowtie antenna capable of supporting next-generation wireless systems. Key performance metrics, including return loss (S11), gain, radiation pattern, and bandwidth, are evaluated to demonstrate the antenna's suitability for 6G front-end integration. The substrate's stable dielectric constant offers a robust solution for mitigating millimeter-wave losses and maintaining consistent electromagnetic performance. With a substrate height of 1.27 mm, the structure provides a practical compromise between mechanical rigidity, bandwidth, and surface-wave suppression [10].

Antenna design and modelling

1- Bowtie antenna design

The bowtie antenna, usually referred to as (bi-conical / planar V-shaped), is conceptually derived from a classical dipole antenna but with flared triangular arms to widen the bandwidth. The geometry covering the arm length L, Flare angle θ, Gap width (g), and Arm width (W). The arm length could be calculated by using the formula in equation 1

$$L \approx \frac{\lambda_0}{4\sqrt{\varepsilon_{eff}}} \quad (1)$$

For arm length

$$L_{arm} \approx \frac{\lambda_0}{4} \quad (2)$$

Total overlap (vertex-to-vertex) is then roughly

$$L_{\text{total}} \approx \lambda_g/2 \quad (3)$$

The antenna layout was constructed as two identical triangular arms extended symmetrically around the feed point, the 2-D top view in ANSYS HFSS environment and 3-D are shown in figure 1 a and b, this antenna is known for Its Wide impedance bandwidth, Stable radiation

pattern and High radiation efficiency, in this type of antennas Increasing the flare angle increases broadband behavior and lowers input impedance; smaller angles narrow the bandwidth and raise input impedance. Sweeping this angle will lead to improving the desired bandwidth. Moreover, the arm width. Wider arms and a broader triangular base increase the radiating area and broaden the bandwidth. However, too wide a range reduces peak gain and shifts the resonance frequency to another goal.

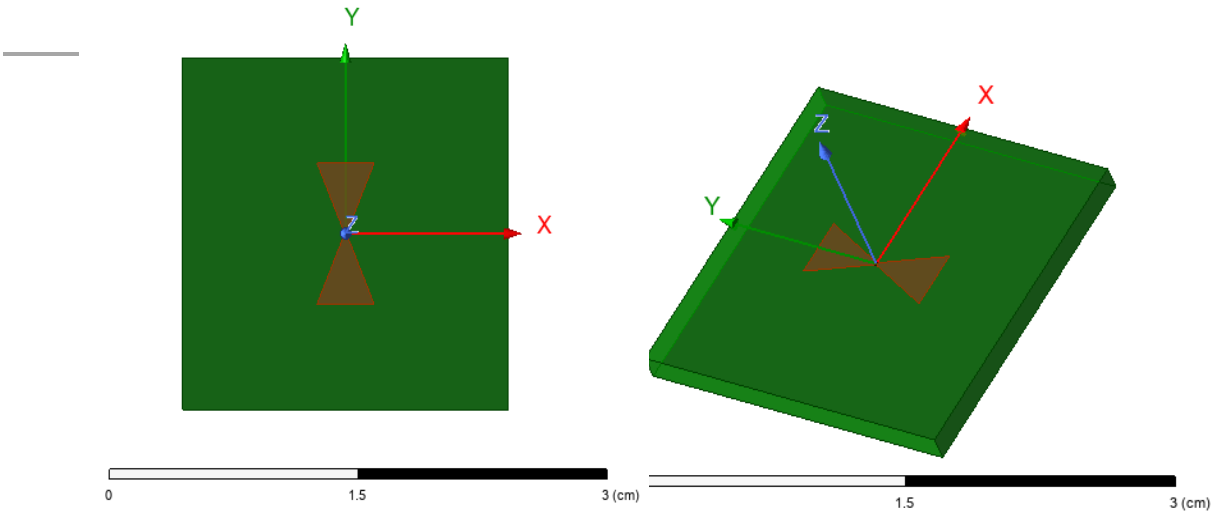

Figure 1. a Bowtie Antenna top view, b- Bowtie Antenna 3-D view.

For our design, a single-element planar bow-tie antenna has been designed with a resonant frequency of 10.0 GHz on a Rogers RT/duroid substrate with relative permittivity ε_r= 2.2 and substrate thickness h = 0.127 mm. The antenna should be compatible with standard PCB fabrication (copper cladding) and simulated /measured with a 50-Ω feed. Antenna dimensions are illustrated in figure 2, we classify the arm lengths into six parts starting with L_1 which indicates the length of the upper triangular arm, L_2 referring to the diagonal edge of the triangle and L_3, L_4, L_5, L_6 represent side lengths around the upper and lower flared sections Where $L_1 = L_2 = 0.35\ cm$ and $L_3 = L_4 = L_5 = L_6 = 0.42\ cm$

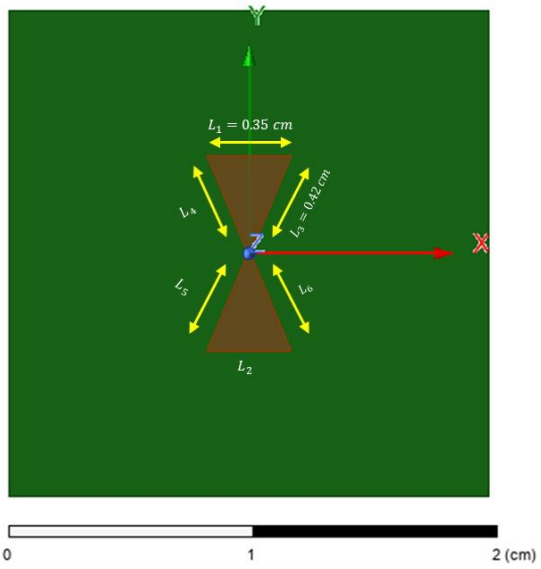

Figure 2. antenna with dimensions $L_1, L_2, L_3, L_4, L_5, L_6$

Figure 3 shows the realized gain distribution projected onto the surface of the bow-tie antenna and its surrounding 3-D radiation envelope at 10 GHz. The gain pattern exhibits the typical characteristics of a planar dipole-type radiator, where radiation is strongest in directions perpendicular to the antenna plane and weaker along the axis aligned with the feed gap. The 3-D gain envelope forms a shape close to an oblate spheroid, indicating a predominantly broadside radiation pattern. This is typical of symmetric bow-tie or dipole antennas, where the majority of radiated power is directed away from the substrate surface, normal to the antenna plane

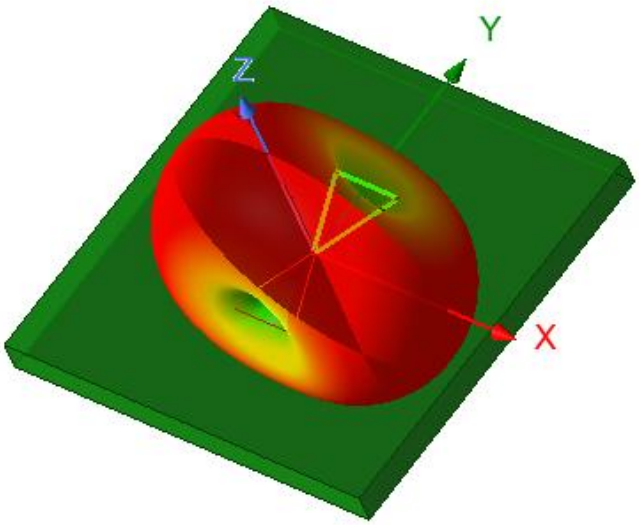

Figure 3. Gain on the antenna body.

Figure 4 indicating an antenna scattering parameter S_{11} the matching of this antenna is accomplished at the design region around 10 GHz (S_{11}< −15 dB), that is the power delivery from the source to the radiator has been realized near the center frequency in this case the antenna is suitable according to 6G test bands around 10 GHz. The fractional bandwidth is approximately 16% where this bandwidth is fairly wide for a single-element bowtie: it will cover a multi-hundred-MHz channel allocation around 10 GHz without additional matching networks. Whether it is sufficient depends on the specific 6G channel bandwidth requirements This antenna comes with a Resonant (minimum) S_{11}approximately -16.5 dB at about 10.36 GHz (deepest point of the trough). The bandwidth is from 9.536 GHz to 11.189 GHz, so we can calculate the absolute BW for 1.653 GHz.

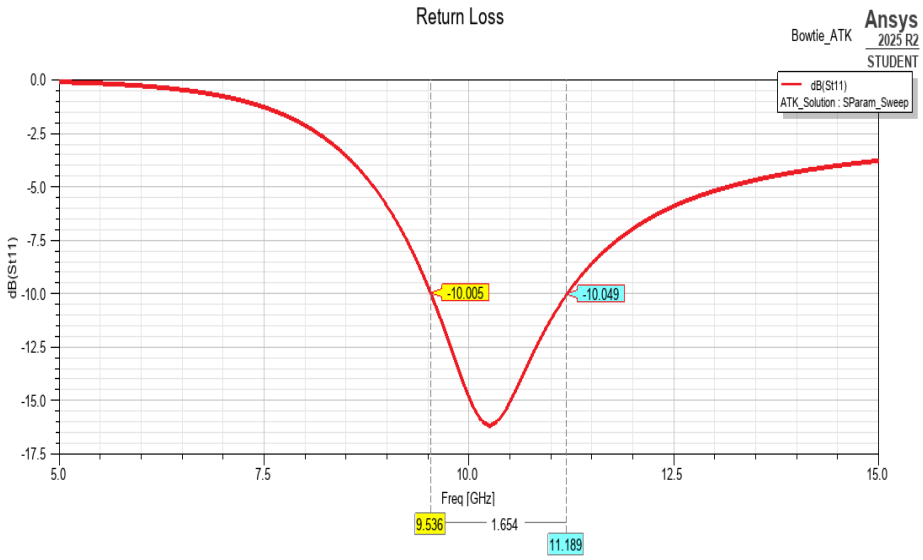

Figure 4. antenna return loss S_{11}

The surface current distribution of the bowtie antenna at 10 GHz is shown in Figure 5, which demonstrates that the strongest currents are concentrated along the feed region and the inner edges of the triangular bow-shaped radiating arms. The plot indicates current magnitudes reaching up to approximately 95 A/m, with the highest intensity shown in red around the feed point, where the excitation is applied. This region exhibits strong electric field coupling and charge acceleration, characteristic of the fundamental resonant mode. As the current propagates outward along each triangular arm, its magnitude gradually decreases, transitioning through orange, yellow, green, and finally blue regions near the arm tips. This smooth current decay confirms efficient radiation, as the bowtie shape supports a wide current flare-out path that enhances broadband performance. The ground plane beneath the antenna shows comparatively low-level surface currents, represented mostly in dark green and blue, indicating that most of the radiated energy originates from the bowtie arms rather than large induced currents on the substrate surface. The symmetry of the current distribution across both arms further verifies proper impedance matching and balanced operation of the bowtie geometry. Overall, the current distribution illustrates strong localization around the feed gap, effective flare-out of currents along each bowtie arm, and minimal unwanted current spreading across the substrate, confirming good radiation efficiency and correct excitation of the intended resonant mode at 10 GHz.

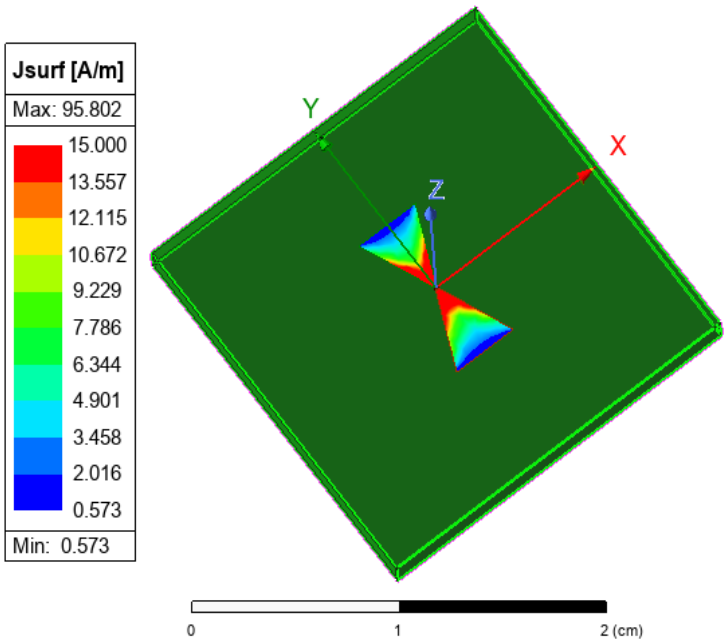

Figure 5. Surface current distribution

Figure 6 illustrates the 2D far-field gain patterns of the proposed antenna at 10 GHz for two angles $\phi = 0°$ and $\phi = 90°$. The results provide insight into the antenna's radiation behavior in the orthogonal planes.

In the $\phi = 0°$ plane, the antenna exhibits an almost circular and uniform radiation profile, indicating stable gain across the full azimuthal range. The maximum gain in this plane is approximately 5–6 dB, with no deep nulls, confirming that the structure supports a relatively omnidirectional radiation characteristic in this cut. This response is typical for antennas with symmetrical transverse geometries where the E-plane maintains consistent radiation.

Conversely, the $\phi = 90°$ plane presents a distinct bi-lobed (figure-eight) radiation pattern. The gain reaches similar peak values of about 5–6 dB, but significant attenuation is observed at the broadside direction, where the gain drops to nearly –15 dB, forming a deep null. This behavior indicates a strong directional sensitivity and suggests that the antenna supports two main lobes oriented in opposite directions along this plane. Such a pattern is commonly associated with dipole-like current distribution or asymmetry within the antenna geometry.

Overall, the combination of an omnidirectional pattern in one plane and a figure-eight pattern in the orthogonal plane demonstrates that the antenna provides polarization- and plane-dependent radiation characteristics. This dual-behavior response is particularly beneficial in applications requiring diversity or multi-directional coverage while maintaining acceptable gain performance at the operating frequency of 10 GHz.

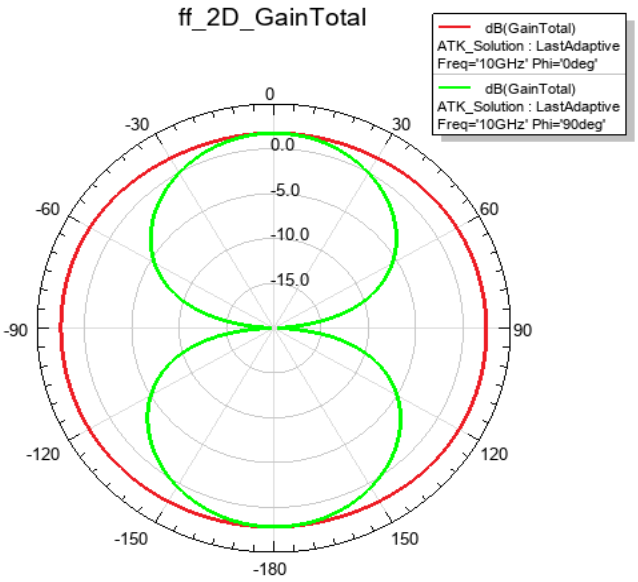

Figure 6. 2-D gain at 10 GHZ for 0 and 90 degrees.

The three–dimensional gain distribution of the proposed antenna is illustrated in Figure 7. The pattern exhibits a predominantly unidirectional radiation behavior, with the highest gain concentrated along the main lobe. The simulated maximum gain reaches approximately 2.6 dBi, indicating that the antenna provides moderate directivity suitable for compact high-frequency applications.

The gain surface shows a smooth, nearly rotationally symmetric shape, suggesting that the antenna maintains stable radiation over a wide angular region. The dominant radiation lobe is identified by the area with maximum gain levels, representing gain levels from 0 to 5 dB, while the backside radiation is significantly suppressed, with minimum gain values dropping to approximately –19.7 dB. This strong front-to-back contrast confirms the antenna's efficiency in concentrating power toward the desired direction while minimizing unwanted radiation.

Furthermore, the transition between high-gain and low-gain regions is gradual, indicating low side-lobe levels and good overall radiation quality. Such a pattern is highly desirable for radar, sensing, and point-to-point communication systems, where stable angular coverage and reduced interference are required. Overall, the obtained 3D gain response verifies that the antenna achieves effective directional radiation performance at the intended operating frequency.

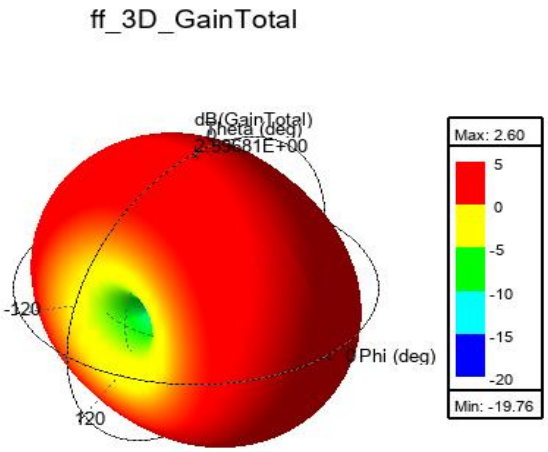

Figure 7. A 3-D antenna gain

The simulated Voltage Standing Wave Ratio (VSWR) of the proposed antenna across the 5–15 GHz frequency range is presented in Figure 8. The antenna demonstrates excellent impedance matching around the target operating band. At the center frequency of 10 GHz, the VSWR reaches approximately 1.44, indicating a strong impedance match and efficient power transfer between the feed line and the radiating structure. The bandwidth in which the VSWR remains below the commonly accepted threshold of 2 extends from approximately 9.54 GHz to 11.19 GHz, providing a fractional bandwidth suitable for wideband and high-frequency communication applications. Within this interval, the antenna maintains low reflection and stable impedance characteristics, confirming its suitability for reliable RF performance. Outside the matched band, the VSWR increases progressively as the operating frequency diverges from resonance, reflecting the expected deterioration in impedance matching. Overall, the obtained VSWR curve verifies that the antenna exhibits good broadband matching, minimized return loss, and efficient operation throughout its intended frequency region.

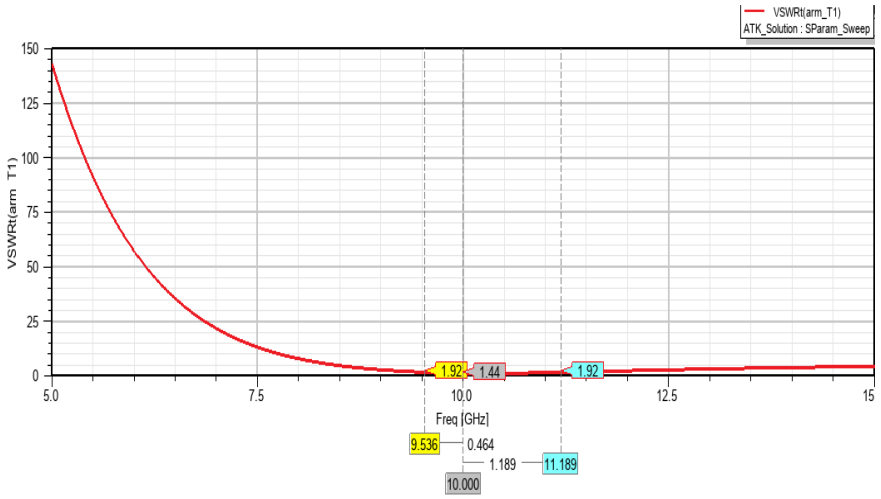

Figure 8. Voltage Standing Wave Ratio VSWR

2-The slot Bow slot antenna

The bowtie slot antenna is shown in Figure 9. Compared to our initial design, this antenna exhibited improved performance. in this design, the same substrate and thickness were used. For this, it's too simple to compare the performance. In the case of scattering parameter S_{11} the slot antenna resonant bandwidth is wider with a ratio of 18 % compared to 16% for the first antenna. the differences between the two antennas in terms of antenna parameters will be tabulated in Table 1.

Libyan Open University Journal of Applied Sciences (LOUJAS)
Volume 1 - Issue 2 - 2025 - Pages 66-76

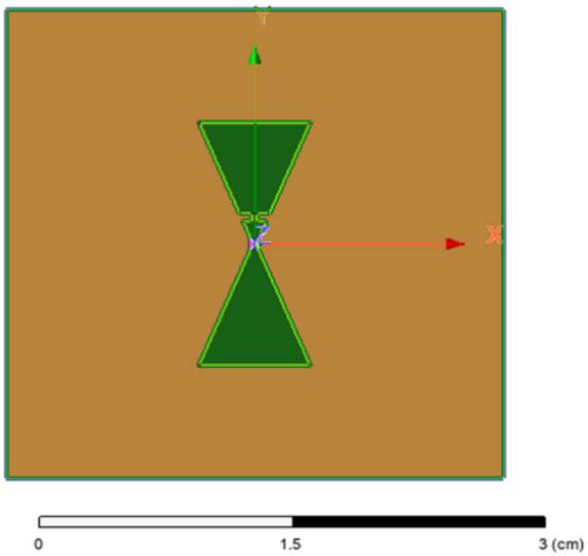

Figure 9. Bowtie slot antenna.

In Figure 10, the reflection coefficient (s_{11}) of the proposed BowtieSlot antenna was evaluated across the 5–15 GHz frequency range to assess its impedance matching characteristics. The antenna exhibits a pronounced resonance at 10 GHz, where the minimum s_{11} reaches −17.018 dB. This value indicates excellent impedance matching, corresponding to a reflected power of less than 2%, meaning that more than 98% of the incident power is effectively delivered to the antenna. Such a low return loss at the target operating frequency confirms that the antenna is well-tuned for efficient radiation at 10 GHz.

In addition to the primary resonance, the antenna maintains s_{11}values below −10 dB over a broad portion of the spectrum, demonstrating its inherent wideband behavior. This wideband impedance performance is particularly advantageous for emerging 6G communication systems, which require antennas capable of supporting high data rates, low latency, and robust spectral efficiency across extended frequency ranges. The results confirm that the inclusion of a slot in the Bowtie structure enhances both the matching level and the usable operational bandwidth. The Bowtie-Slot antenna, therefore, offers improved performance for wideband applications centered at 10 GHz, where enhanced impedance stability and broader spectral coverage are required.

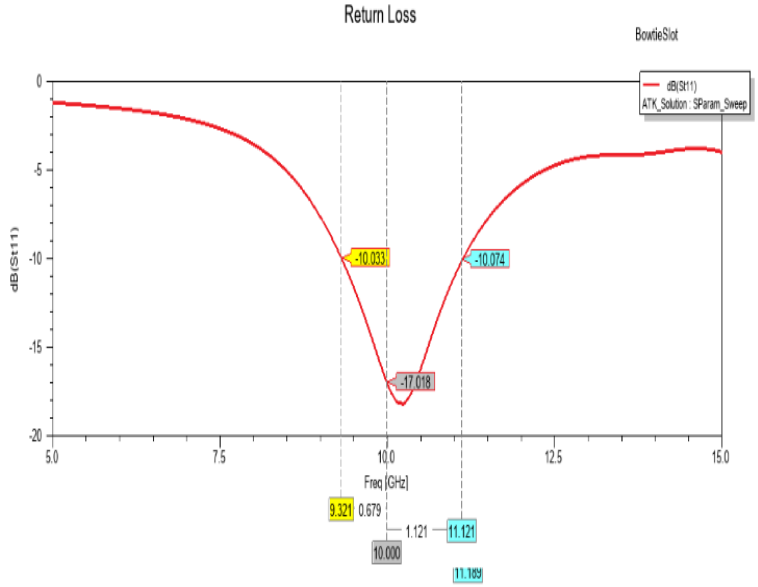

Figure 10. Bowtie slot antenna scattering parameter S_{11}

the Bowtie Slot antenna demonstrates a higher peak gain of 5.68 dBi, as observed in the 3D radiation pattern simulation in Figure 11. This suggests better directional performance and higher radiation efficiency, which are critical for beamforming and spatial multiplexing in 6G networks. The Bowtie antenna, while slightly lower in gain at 2.6 dBi, offers a broader radiation pattern, which may be advantageous for coverage-based applications or mobile platforms. Both antennas maintain planar geometries and wideband impedance characteristics, making them suitable for integration into compact 6G devices.

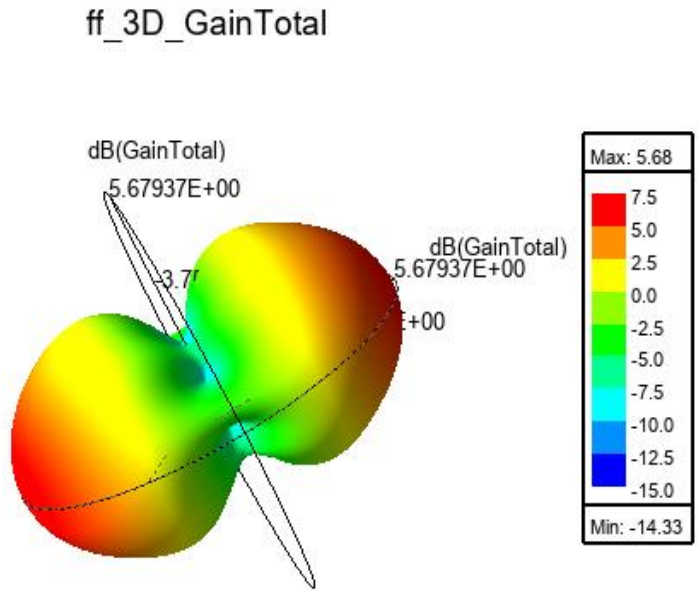

Figure 11. Bowtie slot antenna gain

Table 1 presents a performance comparison between the conventional Bowtie antenna and the modified Bowtie Slot antenna at 10 GHz. The results indicate that the Bowtie Slot design provides notable improvements across most key parameters. The reflection coefficient S_{11} is enhanced from –14.8 dB in the Bowtie to –17 dB in the Bowtie Slot, indicating better impedance matching and lower return loss. The gain also increases significantly from 2.6 dB to 5.68 dB, demonstrating that the slot modification contributes to stronger radiation and improved directivity. The VSWR is reduced from 1.44 to 1.239, confirming superior matching with the transmission line and more efficient power transfer in the slot antenna. Additionally, the bandwidth increases from 16% to 18%, showing that the Bowtie Slot achieves broader operational frequency coverage. Overall, the Bowtie Slot antenna outperforms the standard Bowtie configuration in terms of matching, gain, and bandwidth, making it more suitable for high-performance microwave applications

Table 1. A performance comparison between the conventional Bowtie antenna and the modified Bowtie Slot antenna at 10 GHz.

Antenna Type	Bowtie Antenna	Bowtie Slot Antenna
Peak Gain at 10 GHz	2.6 dBi	5.68 dBi
Radiation Pattern Characteristics	Broad main lobe, moderate directivity	Symmetric 3D lobed pattern, higher directivity
Suitability for 6G	Good for wideband, moderate gain applications	Excellent for directional 6G links
S_{11} at 10 GHz	-14.8 dB	-17 dB
VSWR	1.44	1.239
BW	16%	18%

Conclusion

This work presented the design, simulation, and performance assessment of a compact bowtie antenna operating at 10 GHz for emerging 6G wireless communication applications. Using a Rogers RT/Duroid substrate (with a dielectric constant ε_r of 2.2 and a height of 1.27 mm), the antenna achieved stable broadband performance, good impedance matching, and efficient radiation characteristics suitable for millimeter-wave operation. Full-wave EM simulations confirmed that the bowtie shape supports a wide impedance bandwidth of approximately 16%, with a return loss reaching –16.5 dB at resonance and a usable frequency range from 9.53 GHz to 11.18 GHz. The antenna also showed a maximum realized gain of about 2.6 dB, with radiation primarily directed in the broadside direction.

Surface current analysis confirmed the proper excitation of the fundamental radiating mode, showing strong current concentration near the feed gap and smooth distribution along the triangular arms. The 2D far-field patterns demonstrated a nearly omnidirectional response in the $\phi = 0°$ plane and a bi-lobed dipole-like pattern in the $\phi = 90°$ plane, indicating polarization-dependent radiation behavior.

A comparison with a modified bowtie slot antenna showed that the slot structure provides a slightly wider bandwidth (18%), and the gain level increased to 5.68 dB with a good impedance matching quality, making it an attractive alternative for wider-band 6G channels.

Overall, the results confirm that the proposed bowtie antenna and its slot-enhanced variant are strong candidates for compact 6G front-end modules, short-range high-capacity links, and portable millimeter-wave sensing systems.

References:

1. Balanis, C. A. (2016). *Antenna theory: Analysis and design* (4th ed.). Wiley.
2. Garg, R., Bhartia, P., Bahl, I., & Ittipiboon, A. (2001). *Microstrip antenna design handbook*. Artech House.
3. Wong, K. L. (2003). *Planar antennas for wireless communications*. Wiley.
4. Kumar, G., & Ray, K. P. (2003). *Broadband microstrip antennas*. Artech House.

5. Pozar, D. M. (1992). Microstrip antennas. *Proceedings of the IEEE, 80*(1), 79–91. https://doi.org/10.1109/5.119568
6. Volakis, J., Chen, C.-C., & Fujimoto, K. (2010). *Small antennas: Miniaturization techniques & applications*. McGraw-Hill.
7. Sharma, S. K., & Best, S. R. (2010). A bowtie antenna for wideband applications: Design, analysis, and performance. *IEEE Antennas and Propagation Magazine, 52*(5), 80–88. https://doi.org/10.1109/MAP.2010.5687518
8. Mailloux, R. J. (2018). *Phased array antenna handbook* (3rd ed.). Artech House.
9. Rappaport, T. S., Xing, Y., Kanhere, O., Ju, S., Madanayake, A., Mandal, S., … Zhang, X. (2019). Wireless communications and applications above 100 GHz: Opportunities and challenges for 6G and beyond. *IEEE Access, 7*, 78729–78757. https://doi.org/10.1109/ACCESS.2019.2921522
10. Yahya Entiefa Mansour, Abduladeem Beltayib, & Allafi Omran. (2025). *A Compact F-Slot-Enhanced PIFA Design for Dual-Band Bluetooth and WLAN Applications*. African Journal of Advanced Pure and Applied Sciences, 4(4), 669–675.
11. ANSYS Inc. (2025). *ANSYS HFSS 2025 R2 user guide*. ANSYS Inc.